Constraints on the composition of the Aleutian arc lower crust from V_P/V_S

Donna J. Shillington,[1] Harm J. A. Van Avendonk,[2] Mark D. Behn,[3] Peter B. Kelemen,[1] and Oliver Jagoutz[4]

Received 10 December 2012; revised 15 March 2013; accepted 15 March 2013; published 7 June 2013.

[1] Determining the bulk composition of island arc lower crust is essential for distinguishing between competing models for arc magmatism and assessing the stability of arc lower crust. We present new constraints on the composition of high P-wave velocity (V_P = 7.3–7.6 km/s) lower crust of the Aleutian arc from best-fitting average lower crustal V_P/V_S ratio using sparse converted S-waves from an along-arc refraction profile. We find a low V_P/V_S of ~1.7–1.75. Using petrologic modeling, we show that no single composition is likely to explain the combination of high V_P and low V_P/V_S. Our preferred explanation is a combination of clinopyroxenite (~50–70%) and alpha-quartz bearing gabbros (~30–50%). This is consistent with Aleutian xenoliths and lower crustal rocks in obducted arcs, and implies that ~30–40% of the full Aleutian crust comprises ultramafic cumulates. These results also suggest that small amounts of quartz can exert a strong influence on V_P/V_S in arc crust. **Citation:** Shillington, D. J., H. J. A. Van Avendonk, M. D. Behn, P. B. Kelemen, and O. Jagoutz (2013), Constraints on the composition of the Aleutian arc lower crust from V_P/V_S, *Geophys. Res. Lett.*, *40*, 2579–2584, doi:10.1002/grl.50375.

1. Introduction

[2] Competing models for arc magmatism make different predictions for the thickness and composition of arc lower crust [e.g., *DeBari and Sleep*, 1991]. Information on the composition of arc lower crust is also needed to estimate its long-term stability [*Jull and Kelemen*, 2001; *Behn and Kelemen*, 2006]. To reconcile the average "andesitic" composition of continental crust with primitive island arc compositions, many models call for foundering of dense mafic-ultramafic cumulates into the underlying mantle [e.g., *Arndt and Goldstein*, 1989; *Kay and Kay*, 1993].

[3] However, constraining the composition of the island arc lower crust and distinguishing high-velocity lower crust from upper mantle rocks is difficult because (1) lower crustal arc sections are poorly represented in obducted sections [*Kelemen et al.*, 2003a and references therein]; (2) the primary constraints on the lower crust and upper mantle in many active arcs are xenoliths and P-wave velocities (V_P). It is unclear how representative the former may be, and the latter cannot uniquely distinguish between the effects of composition, temperature and melt. For example, V_P of 7.x km/s beneath the Izu-Bonin-Marianas arc are interpreted to represent hot mantle, possibly with melt [*Suyehiro et al.*, 1996] or ultramafic cumulates [*Kodaira et al.*, 2007]. Even in the absence of elevated temperatures and/or melt, V_P cannot be used to differentiate between different possible lower crustal compositions [e.g., between garnet bearing and plagioclase-free compositions, *Behn and Kelemen*, 2003; *Müntener and Ulmer*, 2006] and/or serpentinized peridotite [e.g., *Lizarralde et al.*, 2002].

[4] Ambiguity in constraining the composition of the deep parts of island arcs with seismic velocities can be reduced by incorporating information on S-wave velocity (V_S) and V_P/V_S ratios [e.g., *Christensen*, 1996]. Here, we combine an analysis of sparse S-wave data from the central Aleutian arc and petrologic modeling to better constrain the composition of the lower crust.

1.1. Existing Constraints on Compositions in the Central Aleutian Arc

[5] Aleutian volcanic rocks exhibit a spectrum of compositions (high-Al basalts, high-Mg basalts, and andesites) and fractionation trends (calc-alkaline and tholeiitic); this compositional diversity has been attributed to variations in fractionation depth, state of stress in the overriding plate, differences in parental magma compositions, and water content [*Kay et al.*, 1982; *Myers*, 1988; *Singer and Myers*, 1990; *Miller et al.*, 1992; *Sisson and Grove*, 1993a; *Kelemen et al.*, 2003b; *Zimmer et al.*, 2010]. These models make different predictions for lower crustal composition. For example, one explanation for the abundance of high-Al basalts is the crystallization of a thick sequence of pyroxenite at depth (possibly due to the presence of water), which would enrich the remaining liquid in Al [*Sisson and Grove*, 1993a]. The mineral assemblages of lower crustal rocks may also be modified following crystallization by metamorphism, particularly the formation of garnet [*Behn and Kelemen*, 2006]. The only direct information on the Aleutian lower crust comes from limited xenoliths, many of which are (olivine-) clinopyroxenites [*Conrad et al.*, 1983; *DeBari et al.*, 1987; *Yogodzinski and Kelemen*, 2007], but it is not clear how representative these are.

[6] Existing active-source seismic data from the Central Aleutians acquired in 1994 with the R/V *Maurice Ewing* and onshore/offshore seismometers (Figure 1) indicate relatively high V_P in the lower crust of the Aleutian arc [*Holbrook et al.*, 1999; *Lizarralde et al.*, 2002; *Shillington et al.*, 2004; *Van Avendonk et al.*, 2004]. For the lower crust of the oceanic island arc, these range from ~7.0–7.1 km/s

Additional supporting information may be found in the online version of this article.

[1]Lamont-Doherty Earth Observatory of Columbia University, Palisades, New York, USA.
[2]Institute for Geophysics, University of Texas, Austin, Texas, USA.
[3]Woods Hole Oceanographic Institution, Woods Hole, Massachusetts, USA.
[4]Massachusetts Institute of Technology, Boston, Massachusetts, USA.

Corresponding author: D. J. Shillington, Lamont-Doherty Earth Observatory of Columbia University, Palisades, NY USA. (djs@ldeo.columbia.edu)

0094-8276/13/10.1002/grl.50375

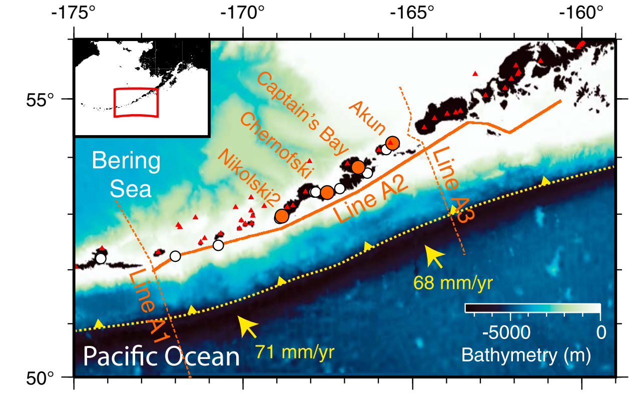

Figure 1. Map with 1994 Aleutian experiment. Bold orange line shows shotline used in this study. Instruments shown with white circles; instruments whose data are used here shown with orange circles and text. Red triangles indicate volcanoes from the Smithsonian Global Volcanism Program. Plate boundary and convergence directions and rates with respect to North American shown with yellow dotted lines, arrows and text [*DeMets et al.*, 2010].

directly beneath the active arc [*Holbrook et al.*, 1999] to 7.3–7.6 km/s slightly trenchward [*Shillington et al.*, 2004]. There is a sharp step in velocity at the top of the lower crust (~0.4 km/s), and along-arc variations in lower crustal velocity appear to correlate to variations in lava composition [*Shillington et al.*, 2004]. These characteristics were attributed to mafic/ultramafic cumulates and/or garnet granulites in the lower crust [*Shillington et al.*, 2004], but V_P alone cannot distinguish between different possible lower crustal compositions and other explanations, such as partial melt in the subarc mantle or serpentinized mantle in the forearc mantle wedge.

1.2. Analysis of *S*-wave Arrivals

[7] To constrain the V_P/V_S ratio of the deep Aleutian arc crust, we performed a very simple analysis of sparse converted *S*-wave arrival times from the arc-parallel wide-angle seismic profile acquired in 1994. Seismometers on the Aleutian Islands recorded shots from the 8000 in^3 airgun array of the R/V *Maurice Ewing*, which steamed south of the islands (Figure 1). Thus, the majority of *P*- and *S*-wave ray paths in this experiment sampled the arc crust trenchward of the active arc, but were still within the arc platform [*Shillington et al.*, 2004; *Van Avendonk et al.*, 2004].

[8] We focus our analysis on arrivals from four stations where converted *S*-wave reflections and refractions were observed at large enough shot-receiver offsets to sample much of the crust (Figure 1). Arrivals occur over source-receiver offsets of 20–180 km and have apparent velocities from ~3 to 4.2 km/s (Figure 2). Consistent with the observation of distinct *P*-wave reflections and refractions from three laterally continuous layers, we identify three crustal *S*-wave refractions with distinct apparent velocities; intracrustal and Moho *S*-wave reflections are also observed (Figure 2 and auxiliary material). Upper crustal arrivals have comparatively 3-D paths due to the experiment geometry, but the longer ray paths of lower crustal refractions and Moho reflections approximately fall in the 2-D plane along the arc platform (Figure 1). Our analysis included 2306 picks; they have large uncertainties (~150–500 ms) because they occur in the coda of the *P*-wave arrivals. Raytracing tests suggest that *P*-to-*S* conversions occurred at the seafloor or at the top of basement beneath a thin veneer of sediments.

[9] *S*-wave arrivals were previously identified in this data set by *Fliedner and Klemperer* [1999], who used travel times in independent 3-D *P*- and *S*-wave tomographic inversions. We argue that the paucity of *S*-wave observations and large uncertainties in travel time picks favor an alternate, simpler analysis approach. We searched for the best-fitting, constant V_P/V_S ratio for each layer. An *S*-wave model was calculated from the *P*-wave model for each of a range of V_P/V_S ratios. We traced rays through each model in 3-D to produce predicted arrivals times for reflections and refractions, which were used to calculate a RMS misfit. Starting with the upper crust and working down, we found the best-fitting constant V_P/V_S ratio for each layer. A fixed delay of 1.8 s was used to account for structure beneath the stations; a similar approach was used for the P-wave modeling [*Van Avendonk et al.*, 2004].

1.3. Results of *S*-wave Modeling

[10] This approach yielded ranges of best-fitting constant V_P/V_S for the upper, middle and lower crust along the central Aleutian island arc. Here we focus on results for the lower crust. The RMS misfit curve for *S*-wave refractions within the lower crust and reflections off the base of the lower crust (i.e., the Moho) shows a clear minimum at a V_P/V_S of 1.70 (Figure 3). Given the large uncertainties associated with travel time picks of these sparse data and the simple approach taken here, models with V_P/V_S between ~1.65

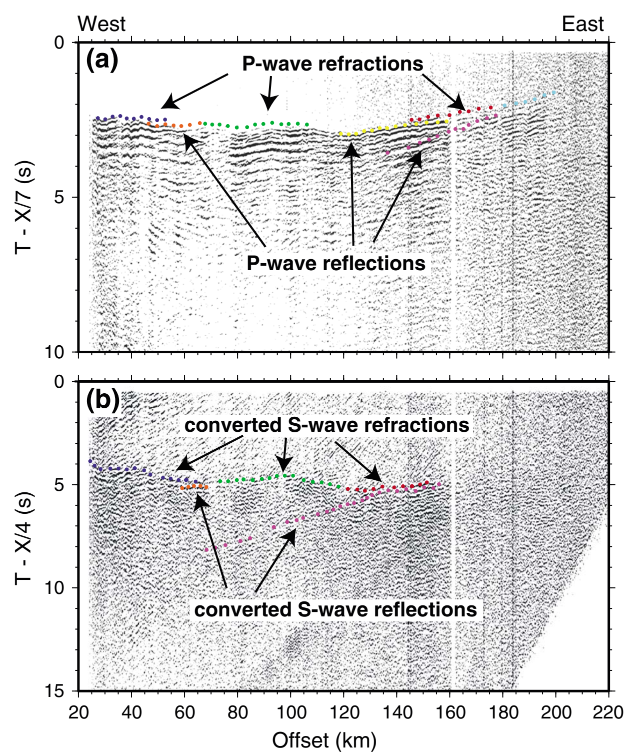

Figure 2. Data from Nikolski2 (location in Figure 1). (a) *P*-wave arrivals in section reduced at 7 km/s. (b) Converted *S*-wave arrivals in same data reduced at 4 km/s. Refractions from upper (blue), middle (green), lower crust (red), and upper mantle (turquoise). Reflections from base of upper (orange), middle (yellow), and lower crust (purple).

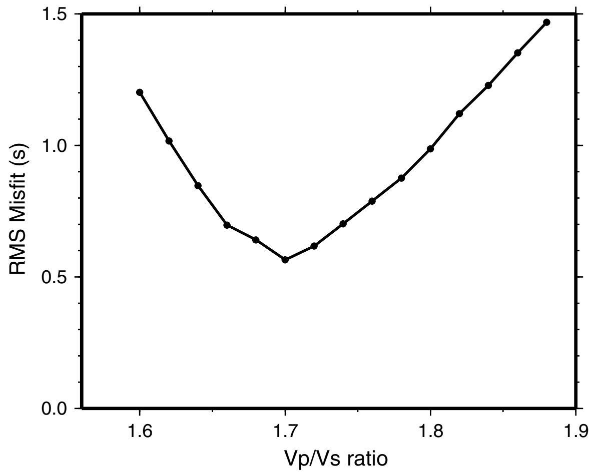

Figure 3. RMS residuals for various lower crustal V_P/V_S for *S*-arrivals on instruments shown in Figure 1.

and 1.75 are considered acceptable. However, the apparent velocities of the refractions, alone, indicate a higher V_P/V_S (~1.75). Additionally, the average lower crustal V_P/V_S based on regional earthquakes indicates a V_P/V_S of ~1.74–1.77 [*Abers*, 1994], and higher lower crustal V_P/V_S are implied in the lower crust directly beneath the active arc by receiver functions at stations along the arc (H. A. Janiszewski *et al.*, 2013, submitted). Thus, we favor the upper end of our acceptable range (1.7–1.75).

1.4. Interpretation of V_P/V_S

[11] The new V_P/V_S results presented here combined with the V_P model along the same profile [*Shillington et al.*, 2004; *Van Avendonk et al.*, 2004] provide unique new constraints on island arc lower crust. Below we discuss different possible explanations for our observations.

[12] Although the range of permissible average V_P/V_S ratios from our study is large, it immediately excludes many possible explanations for 7.*x* km/s *P*-wave velocities in the lower crust and/or upper mantle. If *P*-wave velocities of 7.3–7.6 km/s were caused by serpentinization of the mantle wedge approaching the forearc, we would expect relatively high V_P/V_S [e.g., *Christensen*, 2004, Figure 4]. Likewise, high temperatures and the presence of melt would also increase V_P/V_S [e.g., *Faul and Jackson*, 2005]. Anisotropy can also influence the estimation of V_P/V_S [*Hacker and Abers*, 2012]. However, for the ray paths in this study and possible mineral assemblages in the lower crust, we infer that anisotropy is unlikely to completely account for the observed low V_P/V_S.

[13] In general, the dominant compositional control on V_P/V_S variations in the crust is silica content; higher silica rocks are generally associated with lower V_P/V_S [*Christensen*, 1996, Figure 4]. However, in mafic and ultramafic rocks with low SiO_2, other minerals begin to play a role in controlling the velocity characteristics. There are several possible constituent minerals that could be present in the Aleutian lower crust that would result in a relatively low V_P/V_S (<1.75).

[14] Pyroxenite can have V_P/V_S ranging from ~1.68 to 1.85 (Figure 4), depending on the composition of the pyroxenite (orthopyroxene has a lower V_P/V_S than clinopyroxene) [*Behn and Kelemen*, 2006]. Many xenoliths from the Aleutians are (olivine-) clinopyroxenites [*Conrad et al.*, 1983; *Conrad and Kay*, 1984; *DeBari et al.*, 1987; *Yogodzinski and Kelemen*, 2007]. The estimated V_P of these compositions based on *Hacker and Abers* [2004] (~7.5–7.8 km/s) is at the upper end of the V_P range for the lower crust from *Shillington et al.* [2004] (7.3–7.6 km/s), but the V_P/V_S ratio (~1.77–1.79) is higher than the values presented here (Figure 4). Thus, another composition must be present in addition to (or instead of) clinopyroxenite.

[15] Orthopyroxene has a lower V_P/V_S ratio and could be present due to the breakdown of olivine plus plagioclase to form clinopyroxene, orthopyroxene, and spinel [*Kushiro and Yoder*, 1966]. Alternatively, metasomatism of olivine-rich rocks by silicious fluids can form orthopyroxene at temperatures above serpentinite stability but below the solidus (~700–1000°C) [*Wagner et al.*, 2008]. Orthopyroxenite could fit our observed V_P and V_P/V_S (Figure 4); however, orthopyroxene is not observed in any of the lower crustal or upper mantle xenoliths from the Aleutians [*Conrad et al.*, 1983; *DeBari et al.*, 1987]. Therefore, although orthopyroxene may be present, we find it unlikely that it forms in sufficient abundances to explain the observed V_P/V_S ratios.

[16] Another possible contribution to low V_P/V_S is the presence of quartz. Quartz is common in felsic and intermediate arc rocks. Its presence in more mafic rocks could occur due to fluxing of silicious material from the slab [*Rossi et al.*, 2006]. Alternatively, the metamorphic reaction of enstatite and plagioclase forms garnet, clinopyroxene and quartz [*Kushiro and Yoder*, 1966]. The abundance of quartz in the deep Aleutian crust is unknown; *Conrad et al.* [1983] reported that a gabbroic xenolith from Adak contains quartz. It is also observed in deep crustal rocks from the obducted Kohistan arc [*Yamamoto*, 1993; *Jagoutz and Schmidt*, 2012], but is not observed in lower crustal gabbronorites in the Talkeetna section [*Kelemen et al.*, 2003a; *Behn and Kelemen*, 2006]. The elastic properties of quartz change dramatically with the transition from alpha to beta quartz; alpha quartz has a much lower V_P/V_S (~1.4) than beta quartz (~1.7) [e.g., *Ohno et al.*, 2006]. The profound effect of the alpha-beta quartz transition is illustrated in Figure 4, which shows V_P and V_P/V_S calculated using Perple_X [*Connolly*, 2005] for rocks from obducted arc sections in Talkeetna and Kohistan at 0.8 GPa (see auxiliary material). Calculations at 750°C lie within the alpha quartz stability field, and rocks with higher SiO_2 trend toward low V_P and low V_P/V_S ratios (Figure 4a). By contrast, velocities calculated at 900°C lie within the beta quartz stability field, and rocks with higher SiO_2 trend toward low V_P and high V_P/V_S (Figure 4b). Our rays sample the lower crust trenchward of the active arc line, where colder temperatures are expected, making the stability of alpha quartz more plausible [*Shen et al.*, 1993].

[17] The sensitivity of the expected mineral assemblages arising from different bulk compositions as a function of temperature and pressure was assessed by examining several possible lower crustal compositions derived from obducted arc sections using Perple_X (see auxiliary material). To satisfy the high V_P in the Aleutian lower crust, the presence of quartz, which has low V_P, would need to be balanced by other components with higher V_P, such as garnet. The pressure-temperature window in which both phases are stable is either nonexistent or very narrow and confined to conditions only present in the lowermost Aleutian crust (Figure S7). Consequently, we conclude that alpha quartz

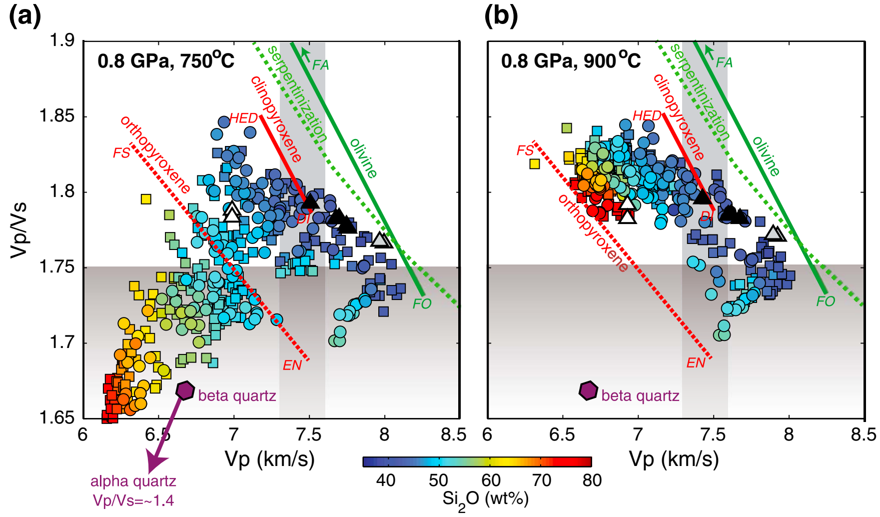

Figure 4. Seismic velocities of obducted arc rocks from Talkeetna and Kohistan [*Kelemen et al.*, 2003a; *Jagoutz et al.*, 2006]. Phase proportions and velocities were calculated from bulk composition with a version of Perple_X modified to include the alpha/beta quartz transition at (a) 750°C and (b) 900°C, which lie in the alpha and beta quartz stability fields, respectively. Squares are ultramafic rocks, and circles are gabbros. We assume gabbros contain 0.5 wt % H_2O and ultramafic rocks are dry. Grey, black, and white triangles are velocities estimated for (olivine-) pyroxenites, dunites, and other compositions (amphibolites and hornblendites) from Aleutian xenoliths, respectively [*DeBari et al.*, 1987] using *Hacker and Abers* [2004]. Grey bands show range of V_P from *Shillington et al.* [2004] and V_P/V_S from this study. Lines and text indicate V_P and V_P/V_S for compositional end-members of olivine (FO-fosterite, FA-fayalite), clinopyroxene (DI-diopside, HED-hedenbergite), and orthopyroxene (EN-enstatite, FS-ferrosillite) from *Hacker and Abers* [2004]. Serpentinite calculated at 600°C. Almost no compositions fall within observed V_P and V_P/V_S ranges for the Aleutian lower crust, suggesting that a mixture of compositions is required.

could contribute to the observed velocity properties of some parts of the crust, but cannot be the sole explanation for the low V_P/V_S ratios over the entire Aleutian lower crust.

[18] Based on the factors discussed above, it does not appear that a single composition can fully explain the V_P and V_P/V_S of the Aleutian lower crust, but rather a combination of rock types is required. We favor the interpretation that there is abundant (olivine-) clinopyroxenite in the Aleutian lower crust, consistent with Aleutian xenoliths. These compositions have V_P that fall within the upper end of the range of V_P observed in the lower crust here, but their estimated V_P/V_S ratios are above the observed range (Figure 4). This requires that other compositions with lower V_P and V_P/V_S must also be present to account for the combination of high V_P and low V_P/V_S. Specifically, we favor mixtures that include compositions with a small amount (<5 wt %) of alpha quartz, such as rocks with ~50–65 wt % SiO_2 (Figure 4). Mixtures with ~30–50% alpha-quartz bearing gabbro (V_P = 7.1 km/s and V_P/V_S = 1.72) and ~50–70% clinopyroxenite (V_P = 7.6 km/s and V_P/V_S = 1.775) could account for our observations.

2. Discussion

[19] We analyzed *S*-wave arrivals to better constrain the composition of the deep part of the Aleutian arc, which includes a thick layer with V_P of 7.3–7.6 km/s [*Shillington et al.*, 2004]. We find relatively low V_P/V_S values of ~1.7–1.75 for this layer, which is consistent with abundant clinopyroxenite (as indicated by Aleutian xenoliths) in addition to another composition with lower V_P and lower V_P/V_S ratios. We favor gabbro or another evolved composition with small amounts (<5%) of alpha quartz. The pressures and temperatures expected across the arc crustal section from the active arc toward the trench span the alpha-beta quartz boundary, such that even small amounts of quartz could result in large changes in V_P/V_S in the middle and lower crust across island arcs.

[20] We use lower crustal V_P and V_P/V_S to estimate that ~50–70% of the lower crust is composed of clinopyroxenite, implying that it forms ~30–40% of the entire Aleutian crustal section. The portion of the Aleutian crust comprising ultramafic cumulates is larger than the proportion of equivalent compositions exposed in obducted arcs, but similar to estimates of their proportions based on geobarometry and mass balances [*Kay and Kay*, 1985; *DeBari and Sleep*, 1991; *Greene et al.*, 2006; *Jagoutz and Schmidt*, 2012]. In contrast to what is interpreted for many other island arcs, we interpret the presence of significant ultramafic cumulates above the seismic Moho, and that our Moho represents the contact between mafic-ultramafic cumulates and mantle. In many arcs, these compositions are inferred to lie beneath the seismic Moho; their high velocities might make them indistinguishable from hot upper mantle, such that the Moho might instead represent a boundary between plagioclase-bearing and ultramafic compositions [*Müntener and Ulmer*, 2006; *Kodaira et al.*, 2007; *Tatsumi et al.*, 2008].

[21] The presence of abundant clinopyroxenite in the Aleutian lower crust can explain several key characteristics of Aleutian lavas. The crystallization of a thick layer of pyroxenite will result in a higher-Al liquid and could account for high-Al basalts in the Aleutians [*Sisson and Grove*, 1993a; *Müntener et al.*, 2001]. Likewise, the

depletion of the remaining melt in Fe could explain calc-alkaline fractionation trends [*Sisson and Grove*, 1993b; *Zimmer et al*., 2010]. The presence of water in the parental magma suppresses plagioclase, which can enable the crystallization of thick sections of pyroxenite and a more abrupt "plag-in" [*Müntener et al*., 2001]. Approximately 3–4 wt % H_2O is estimated for lavas in the oceanic Aleutian arc from melt inclusions [*Zimmer et al*., 2010]. Simple petrological modeling suggests that the suppression of plagioclase crystallization due to the presence of water may partially account for the sharp step in V_P at the top of the lower crust in the Aleutians (Figure S8). However, our interpretation of multiple compositions in the lower crust implies that magmas undergo varied crystallization sequences during their ascent, which may also help explain the compositional diversity observed at volcanoes.

3. Conclusions

[22] The analysis of sparse converted *S*-waves in an along-arc refraction profile in the Aleutian island arc yields low average V_P/V_S ratios for the lower crust. The combination of high V_P and low V_P/V_S is best explained by a combination of abundant clinopyroxenite and another mafic composition containing alpha quartz. This interpretation is consistent with Aleutian xenoliths, obducted arc sections, and many petrological models for Aleutian magmas. Better constraints on *S*-wave velocity in the Aleutians and other arcs can greatly improve our knowledge of arc crustal composition.

[23] **Acknowledgments.** We gratefully acknowledge B. Hacker, G. Abers and H. Janiszewski for discussions, J. Connolly for help with Perple_X, and M. Fliedner and S. Klemperer for providing information on the Aleutians Experiment. PBK's contributions supported by the Arthur D. Storke Chair at Columbia University and by NSF grants OCE 0520378, OCE 0728077, and EAR 0727013. The constructive suggestions of two anonymous reviewers and A. Newman greatly improved the manuscript.

References

Abers, G. A. (1994), Three-dimensional inversion of regional P and S arrival times in the East Aleutians and sources of subduction zone gravity highs, *J. Geophys. Res.*, *99*(B3), 4395–4412.

Arndt, N. T., and S. L. Goldstein (1989), An open boundary between continental crust and mantle: its role in crust formation and crustal recycling, *Tectonophysics*, *161*, 201–212.

Behn, M. D., and P. B. Kelemen (2003), Relationship between seismic P-wave velocity and the composition of anhydrous igneous and meta-igneous rocks, *Geochem. Geophys. Geosys*., *4*(5), 1041, doi:1010.1029/2002GC000393.

Behn, M. D., and P. B. Kelemen (2006), The stability of arc lower crust: Insights from the Talkeetna Arc section, south-central Alaska and the seismic structure of modern arcs, *J. Geophys. Res.*, *111*, B11207, doi:11210.11029/12006JB00427.

Christensen, N. I. (1996), Poisson's ratio and crustal seismology, *J. Geophys. Res.*, *101*(B2), 3139–3156.

Christensen, N. I. (2004), Serpentinites, peridotites, and seismology, *Intern. Geol. Rev.*, *46*, 795–816.

Connolly, J. A. D. (2005), Computation of phase equilibria by linear programming: A tool for geodynamic modeling and its application to subduction zone decarbonation, *Earth Planet. Sci. Lett.*, *236*, 524–541.

Conrad, W. K., S. M. Kay, and R. W. Kay (1983), Magma Mixing in the Aleutian Arc: Evidence From Cognate Inclusions and Composite Xenoliths, *J. Volcanol. Geotherm. Res.*, *18*, 279–295.

Conrad, W. K., and R. W. Kay (1984), Ultramafic and Mafic Inclusions from Adak Island: Crystallization History, and Implications for the Nature of Primary Magmas and Crustal Evolution of the Aleutian Arc, *J. Petrol.*, *25*, 88–125.

DeBari, S., S. M. Kay, and R. W. Kay (1987), Ultramafic xenoliths from Adagdak Volcano, Adak, Aleutian Islands, Alaska: Deformed Igneous Cumulates from the Moho of an Island Arc, *J. Geol.*, *95*, 329–341.

DeBari, S. M., and N. H. Sleep (1991), High-Mg, low-Al bulk composition of the Talkeetna island arc, Alaska: Implications for primary magmas and the nature of arc crust, *Geol. Soc. Am. Bull.*, *103*, 37–47.

DeMets, C., R. G. Gordon, and D. F. Argus (2010), Geological current plate motions, *Geophys. J. Intl.*, *181*, 1–80.

Faul, U. H., and I. Jackson (2005), The seismological signature of temperature and grain size variations in the upper mantle, *Earth and Planetary Science Letters*, *234*, 119–134.

Fliedner, M. M., and S. L. Klemperer (1999), Structure of an island-arc: Wide-angle seismic studies in the eastern Aleutian Islands, Alaska, *J. Geophys. Res.*, *104*(B5), 10667–10694.

Greene, A. R., S. DeBari, P. B. Kelemen, J. Blusztajn, and P. D. Clift (2006), A detailed geochemical study of island arc crust: The Talkeetna Arc Section, South-central Alaska, *J. Petrol.*, *47*(6), 1051–1093.

Hacker, B. R., and G. A. Abers (2004), Subduction Factory 3: An Excel worksheet and macro for calculating the densities, seismic wave speeds, and H_2O contents of minerals and rocks at pressure and temperature, *Geochem. Geophys. Geosys.*, *5*(1), Q01005, doi:01010.01029/02003GC000614.

Hacker, B. R., and G. A. Abers (2012), Subduction Factory 5: Unusually low Poisson's ratios in subduction zones from elastic anisotropy of peridotite, *J. Geophys. Res.*, *117*, B06308, doi:10.1029/2012JB009187.

Holbrook, W. S., D. Lizarralde, S. McGeary, N. Bangs, and J. Diebold (1999), Structure and composition of the Aleutian island arc and implication for continental crustal growth, *Geology*, *27*(1), 31–34.

Jagoutz, O., O. Müntener, J.-P. Burg, P. Ulmer, and E. Jagoutz (2006), Lower continental crust formation through focused flow in km-scale melt conduits: The zoned ultramafic bodies of the Chilas Complex in the Kohistan island arc (NW Pakistan), *Earth Planet. Sci. Lett.*, *242*, 320–342.

Jagoutz, O., and M. W. Schmidt (2012), The formation and bulk composition of modern juvenile continental crust: The Kohistan arc, *Chem. Geol.*, *298–299*, 79–96.

Janiszewski, H. A., G. A. Abers, D. Shillington, and J. A. Calkins (2013), Crustal structure along the Aleutian island arc: New insights from receiver functions constrained by active source data, *Geochem. Geophys. Geosys.*, submitted.

Jull, M., and P. B. Kelemen (2001), On the conditions for lower crustal convective instability, *J. Geophys. Res.*, *106*(B4), 6423–6446.

Kay, R. W., and S. M. Kay (1993), Delamination and delamination magmatism, *Tectonophysics*, *219*, 177–189.

Kay, S. M., R. W. Kay, and G. P. Citron (1982), Tectonic Controls of Tholeiitic and Calc-Alkaline Magmatism in the Aleutian Arc, *J. Geophys. Res.*, *87*(B5), 4051–4072.

Kay, S. M., and R. W. Kay (1985), Role of crystal cumulates and the oceanic crust in the formation of the lower crust of the Aleutian arc, *Geology*, *13*, 461–464.

Kelemen, P. B., K. Hanghøf, and A. R. Greene (2003a), One view of the geochemistry of subduction-related magmatic arcs, with an emphasis on primitive andesite and lower crust, in *The Crust*, edited by R. L. Rudnick, Elsevier, Oxford.

Kelemen, P. B., G. M. Yogodzinski, and D. W. Scholl (2003b), Along-Strike Variation in the Aleutian Island Arc: Genesis of High Mg# Andesite and Implications for Continental Crust, Geophys. Mono. Ser., 138, pp. 223–276.

Kodaira, S., T. Sato, N. Takahashi, A. Ito, Y. Tamura, Y. Tatsumi, and Y. Kaneda (2007), Seismological evidence for variable growth of crust along the Izu intra-oceanic arc, *J. Geophys. Res.*, *112*(B5), B05104.

Kushiro, I., and H. S. Yoder (1966), Anorthite-forsterite and anorthite-enstatite reactions and their bearing on basalt-eclogite transformation, *J. Pet.*, *7*(3), 337.

Lizarralde, D., W. S. Holbrook, S. McGeary, N. Bangs, and J. Diebold (2002), Crustal construction of a volcanic arc, wide-angle seismic results from the western Alaska Peninsula, *J. Geophys. Res.*, *107*(8), 2164, doi:10.1029/2001JB000230.

Miller, D. M., C. H. Langmuir, S. L. Goldstein, and A. L. Franks (1992), The Importance of Parental Magma Composition to the Calc-Alkaline and Tholeiitic Evolution: Evidence From Umnak Island in the Aleutians, *J. Geophys. Res.*, *97*(B1), 321–343.

Müntener, O., P. B. Kelemen, and T. L. Grove (2001), The role of H2O during crystallization of primitive arc magmas under uppermost mantle conditions and genesis of igneous pyroxenites: an experimental study, *Contributions to Mineralogy and Petrology*, *141*, 643–658.

Müntener, O., and P. Ulmer (2006), Experimentally derived high-pressure cumulates from hydrous arc magmas and consequences for the seismic velocity structure of island arc crust, *Geophys. Res. Lett.*, *33*(21), L21308, doi:21310.21029/22006GL027629.

Myers, J. D. (1988), Possible petrogenetic relations between low- and high-MgO Aleutian basalts, *Geol. Soc. Am. Bull.*, *100*, 1040–1053.

Ohno, I., K. Harada, and C. Yoshitomi (2006), Temperature variation of elastic constants of quartz across the alpha-beta transition, *Phys. Chem. Minerals*, *33*, 1–9.

Rossi, G., G. A. Abers, S. Rondenay, and D. H. Christensen (2006), Unusual mantle Poisson's ratio, subduction, and crustal structure in central Alaska, *J. Geophys. Res.*, *111*, B09311, doi:10.1029/2005JB003956.
Shen, A. H., W. A. Bassett, and I.-M. Chou (1993), The alpha-beta quartz transition at high temperatures and pressures in a diamond-anvil cell by laser interferometry, *Am. Mineral.*, *78*, 694–698.
Shillington, D. J., H. J. A. Van Avendonk, W. S. Holbrook, P. B. Kelemen, and M. J. Hornbach (2004), Composition and structure of the central Aleutian island arc from arc-parallel wide-angle seismic data, *Geochem. Geophys. Geosys.*, *5*, Q10006, doi:10.1029/2004GC000715.
Singer, B. S., and J. D. Myers (1990), Intra-arc extension and magmatic evolution in the central Aleutian arc, *Alaska, Geology*, *18*, 1050–1053.
Sisson, T. W., and T. L. Grove (1993a), Temperatures and H_2O contents of low-MgO high-alumina basalts, *Contrib. Mineral Petrol.*, *113*, 167–184.
Sisson, T. W., and T. L. Grove (1993b), Experimental investigations of the role of H_2O in calc-alkaline differentiation and subduction zone magmatism, *Contrib. Mineral Petrol.*, *113*(2), 143–166.
Suyehiro, K., N. Takahashi, Y. Ariie, Y. Yokoi, R. Hino, M. Shinohara, T. Kanazawa, N. Hirata, H. Tokuyama, and A. Taira (1996), Continental crust, crustal underplating, and low-Q upper mantle beneath an oceanic island arc, *Science*, *272*, 390–392.
Tatsumi, Y., H. Shukuno, K. Tani, N. Takahashi, S. Kodaira, and T. Kogisa (2008), Structure and growth of the Izu-Bonin-Mariana arc crust: 2. Role of crust-mantle transformation and the transparent Moho in arc crust evolution, *J. Geophys. Res.*, *113*, B02203, doi:10.1029/2007JB005121.
Van Avendonk, H. J. A., D. J. Shillington, W. S. Holbrook, and M. J. Hornbach (2004), Inferring crustal structure in the Aleutian island arc from a sparse wide-angle seismic dataset, *Geochem. Geophys. Geosys.*, *5*, Q08008, doi:10.1029/2003GC000664.
Wagner, L. S., M. L. Anderson, J. M. Jackson, S. L. Beck, and G. Zandt (2008), Seismic evidence for orthopyroxene enrichment in the continental lithosphere, *Geology*, *36*(12), 935–938.
Yamamoto, H. (1993), Contrasting metamorphic P-T-time paths of the Kohistan granulites and tectonics of the western Himalayas, *J. Geol. Soc. London*, *150*, 843–856.
Yogodzinski, G. M., and P. B. Kelemen (2007), Trace elements in clinopyroxenes from Aleutian xenoliths: Implications for primitive subduction magmatism in an island arc, *Earth Planet. Sci. Lett.*, *256*(3–4), 617–632.
Zimmer, M. M., T. Plank, E. H. Hauri, G. M. Yogodzinkski, P. Stelling, J. Larsen, B. Singer, B. Jicha, C. Mandeville, and C. J. Nye (2010), The Role of Water in Generating the Calc-alkaline Trend: New Volatile Data for Aleutian Magmas and a New Tholeiitic Index, *J. Pet.*, *51*, 2411–2444.